IEEE Access
Multidisciplinary | Rapid Review | Open Access Journal

Received June 22, 2019, accepted July 2, 2019, date of publication July 5, 2019, date of current version July 25, 2019.

Digital Object Identifier 10.1109/ACCESS.2019.2927000

Robust H_∞/S-plane Controller of Longitudinal Control for UAVs

XINGCHENG ZHAO, MEINI YUAN, PENGYUN CHENG, LE XIN, AND LEIBIN YAO
College of Mechatronic Engineering, North University of China, Taiyuan 030051, China

Corresponding author: Meini Yuan (mnyuan@126.com)

This work was supported in part by the National Natural Science Foundation of China under Grant 51775518, in part by the Natural Science Foundation of NUC under Grant 51201155, in part by the Key Laboratory of Aircraft Structural Integrity Technology of the Ministry of Industry and Information Technology, and in part by the Open Fund of Key Laboratory of High Performance Ship Technology (Wuhan University of Technology), Ministry of Education, under Grant gxnc19051802.

ABSTRACT In order to resolve the external disturbances and model parameters uncertainty during the unmanned aerial vehicles flight process, in this paper, we designed the H∞/S-plane controller for longitudinal control of unmanned aerial vehicles (UAVs). The S-plane control model with strong nonlinearity was used as the outer loop controller and the robust $H\infty$ control algorithm with strong robustness was used as the inner loop controller. The effectiveness of the H∞/S-plane controller in the longitudinal control of unmanned aerial vehicles without external interference, with external interference and parameter perturbation, was simulated by a certain UAVs nominal model. The results showed that compared with H∞/PD controller and PID controller, H∞/S-plane controller has faster response speed and stronger anti-interference ability. So H∞/S-plane controller is more suitable for the longitudinal control of unmanned aerial vehicles than H∞/PD controller and PID controller.

INDEX TERMS Unmanned aerial vehicle, robust $H\infty$ control, S-plane control, longitudinal control.

I. INTRODUCTION

With the need of application and the development of aviation technology, unmanned aerial vehicles (UAVs) as a new type of intelligent equipment has been widely concerned and applied in military and civil fields. Compared with manned aircraft, UAVs have the advantages of low loss, low cost, a lower casualty rate, easy maintenance and maneuverability, etc. They can be used in harsh and dangerous environments to accomplish tasks that are difficult for manned aircraft. On the military side [1], [2], UAVs can serve as aerial reconnaissance and weapon platforms, carrying different equipment and equipment to complete various military tasks. In the civil field [3], UAVs can be used for heavy or dangerous tasks such as map mapping, resource exploration, communication relay, artificial rainfall, meteorological detection, environmental monitoring [4], atmospheric [5] and oceanic sampling research, etc [6].

UAVs are required to have good control performance and stability when they are disturbed by the outside world. Good control performance refers to the capability of UAV to rapidly and accurately change and maintain flight speed, direction, altitude and other states, that is, it cannot only quickly adjust flight speed, direction, altitude and others to reach the set value, but also can quickly stabilize at the set value, the over harmonic fluctuation as small as possible. Stability refers to the ability of the UAV to recover to the set value in the face of external disturbances and systematic errors.

The longitudinal control system of UAV is established with the pitch Angle control system as the inner loop control and the flight speed control and altitude control as the outer loop control. At present, the commonly used UAV longitudinal control methods include PID control, incremental dynamic inverse control, fuzzy control [7], neural network control [8], adaptive control approaches and so on. For UAV, a nonlinear and easily interfered controlled object, the traditional PID control is simple and easy to implement, but its anti-interference ability is poor. Sieberling [9] *et al.* adopted incremental nonlinear dynamic inversion (INDI), and demonstrated that INDI has good control effect. However the drones in the process of flight, as the changes of speed, height, load, and the increasing consumption of fuel, the controlled object is a time-varying nonlinear system, and is difficult to accurately describe, which lead to the practical application

The associate editor coordinating the review of this manuscript and approving it for publication was Giovanni Angiulli.

very difficulties of INDI. Fuzzy control needn't accurate mathematical model and has strong robustness, but the control system lacks systematicness and cannot define the control target. Neural network control has strong robustness and nonlinear fitting ability, but the control algorithm is complex, and it is easy to lose information in the control process. Adaptive control approaches is usually mixed with other control methods, and the control algorithm is complex, which is not conducive to engineering implementation. Generally speaking, the simpler the control model is, the higher the control precision and anti-interference ability is, and the more it can meet the needs of UAV as a special carrier.

Compared with other control algorithms, s-plane control algorithm is simpler and has higher control accuracy and anti-interference ability. So we apply the simple model and high precision S-plane control model [10] to the longitudinal control of UAV, and its control model has been widely used in the field of underwater robot [11]. At the same time, the robust model is used to improve it [12], [13], and a method based on H∞/S surface model control is designed to control the longitudinal control system of UAV. The H∞/PD model control and PID control effects are compared to verify the rapidity, accuracy, robustness and dynamic performance of H∞/S-plane model control.

II. LONGITUDINAL FLIGHT OF MATHEMATICAL MODEL

Based on the premise of steady-state flight, this paper decouples the UAV flight motion and linearizes the decoupled nonlinear longitudinal motion by using coefficient freezing method and small disturbance linearization principle. The longitudinal motion equation of small disturbance linearization of aircraft is as follows:

$$\begin{bmatrix} \Delta\dot{V} \\ \Delta\dot{\alpha} \\ \Delta\dot{q} \\ \Delta\dot{\theta} \end{bmatrix} = \begin{bmatrix} X_V & X_\alpha & 0 & -g \\ Z_V & Z_\alpha & 1 & 0 \\ M_V & M_\alpha & M_q & 0 \\ 0 & 0 & 1 & 0 \end{bmatrix} \begin{bmatrix} \Delta V \\ \Delta\alpha \\ \Delta q \\ \Delta\theta \end{bmatrix} + \begin{bmatrix} X_{\delta_e} & X_{\delta_T} \\ Z_{\delta_e} & Z_{\delta_T} \\ M_{\delta_e} & M_{\delta_T} \\ 0 & 0 \end{bmatrix} \begin{bmatrix} \Delta\delta_e \\ \Delta\delta_T \end{bmatrix} \quad (1)$$

where V, α, θ and q respectively represent velocity, angle of attack, pitch angle and pitch angle velocity; $\Delta\delta_e$ and $\Delta\delta_T$ represent the elevator and throttle lever perturbations.

The nominal model adopts the model of aircraft longitudinal motion in the state space:

$$\begin{cases} \dot{x} = Ax + Bu \\ y = Cx + Du \end{cases} \quad (2)$$

The research object of this paper is a certain type of UAV. The aircraft model with longitudinal short period mode is adopted, short period motion refers to the motion described by the moment dynamic equation, and the rudder loop transfer function is:

$$G_\delta(S) = \frac{-20}{s + 20} \quad (3)$$

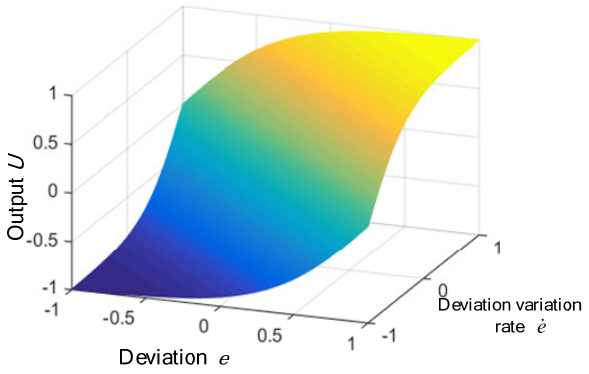

FIGURE 1. Sigmoid surface 3D view.

When the horizontal velocity of the uav is 53.5m/s, the longitudinal motion equation is reflected in equation (2)

$$A = \begin{bmatrix} -0.045 & 1.929 & 0 & -9.81 \\ -0.0071 & -2.02 & 1 & 0 \\ 0.0062 & -6.969 & -2.948 & 0 \\ 0 & 0 & 1 & 0 \end{bmatrix},$$

$$B = \begin{bmatrix} 0 \\ -0.16 \\ -11.87 \\ 0 \end{bmatrix}, \quad C = \begin{bmatrix} 0 & 0 & 0 & 1 \end{bmatrix}, \ D = 0$$

III. H∞/S-PLANE MODEL CONTROL CONCEPT

A. S-PLANE CONTROL METHOD [14], [15]

The control model of S-plane control method is:

$$u = 2.0/(1.0 + e^{(-k1e - k2\dot{e})}) - 1.0 + \Delta u \quad (4)$$

where, k1 and k2 are the control parameters; $\dot{e}$ and e are the deviation and deviation change rate respectively, and this paper is the depth deviation and depth deviation change rate; u is the control output, and Δu is the deviation adjustment item to adapt to environmental disturbance.

The S-plane control is evolved from PD control, and the two have many similarities and differences. The differences between the S-plane control method and PD control can be summarized as the following two points: first, the output of S-plane control has saturation value, which is different from PD control without range limitation. The output range of S-plane control is limited to the range from -1 to $+1$, respectively representing the maximum output in reverse and forward direction. According to this property of S-plane method, when applying this control method, it is necessary to add gain to the output value, namely, multiply u by the maximum output force or torque that can be provided on this degree of freedom, and obtain the output value formula:

$$F_i = K_{u_i} \quad (5)$$

Second, the S-plane controller is more nonlinear. The right figure shows the side of S-plane. It can be seen that when the input range is in the middle of the curve, the output value is small, but the output value has a large rate of change. On the

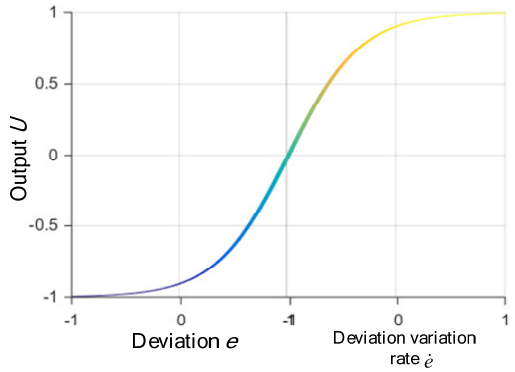

FIGURE 2. Sigmoid surface side view.

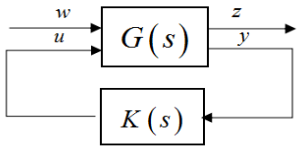

FIGURE 3. $H\infty$ standard design problem.

contrary, if it is at both ends of the curve, the output changes slowly, and the value is relatively large and close to the saturation state. In short, the output value of the S-plane control method is in a non-linear state, contrary to the change rate of the output value. Therefore, the S-plane control method and the improved control algorithm based on it are suitable for the control of such nonlinear controlled objects as UAV.

1) ROBUST $H\infty$ CONTROL METHOD

H_∞ control problem: in the actual control system, H_∞ control problems can be expressed by standard control problems, as shown in Fig.3.

In the figure, w is the external input signal, including external interference, noise, reference input, etc. u is the controller output; z is the controlled output; y is the measured signal; $G(s)$ is the generalized controlled object, including the actual control object and weighting function, and $K(s)$ is the controller to be designed.

The generalized equation of controlled plant is:

$$G(s): \begin{cases} \dot{x} = Ax + B_1 w + B_2 u \\ z = C_1 x + D_{11} w + D_{12} u \\ y = C_2 x + D_{21} w + D_{22} u \end{cases} \tag{6}$$

where, $x \in R^n$ is the n-dimensional state vector of the generalized controlled object, represents the motion variable; $w \in R^{m_1}$ is the m_1 dimension number vector, and $u \in R^{m_2}$, $z \in R^{p_1}$, $y \in R^{p_2}$ are m_2, p_1 and p_2 dimension number vectors respectively; A, B, C and D represents the model matrix element. The above-mentioned formula can also be expressed as:

$$G(s) = \begin{bmatrix} A & B_1 & B_2 \\ C_1 & D_{11} & D_{12} \\ C_2 & D_{21} & D_{22} \end{bmatrix} = \begin{bmatrix} G_{11}(s) & G_{12}(s) \\ G_{21}(s) & G_{22}(s) \end{bmatrix} \tag{7}$$

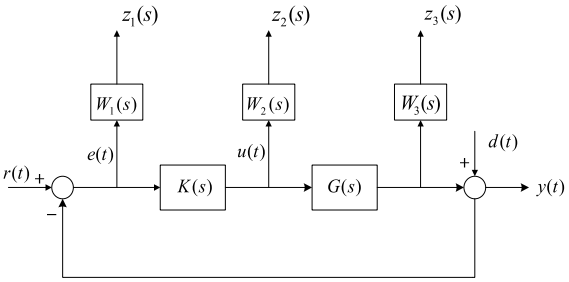

FIGURE 4. Control structure diagram of mixed sensitivity problem.

According to equation (7):

$$G_{ij}(s) = C_i(sI - A)B_j + D_{ij} \tag{8}$$

The closed-loop transfer function from w to z is:

$$G_{zw} = F_l(G, K) = G_{11} + G_{12}K(I - G_{22}K)^{-1}G_{21} \tag{9}$$

The standard H_∞ design problem is to determine whether there is a feedback controller to make the closed-loop transfer function internally stable and make $\|G_{zw}\| < 1$ true for a given generalized controlled object $G(s)$. If it exists, the robust H_∞ controller can be obtained.

Robust H_∞ control for weighted mixed sensitivity problems

Fig.4 shows the control structure of the mixed sensitivity problem. If the control object is a fixed-wing UAV, there are. In the figure, $r(t)$, $e(t)$, $u(t)$, $d(t)$ and $y(t)$ are the reference input, pitching angle error, control input, external interference and system output. $G(s)$ is the controlled object aircraft; K of s is H_∞ infinity controller; $W_1(s)$ is the weight function added at the end of $e(t)$, $W_2(s)$ is the weight function added at the end of $u(t)$, and $W_3(s)$ is the weight function added after the controlled object. Where, the weight function $W_1(s)$ represents the constraint on system performance requirements, and the influence of interference can be effectively suppressed through adjustment to obtain the desired output signal. The weighted function $W_2(s)$ reflects the limit of additive uncertainty. The weighted function $W_3(s)$ reflects the limit of the multiplicative uncertainty.

$W_1(s)$ is the performance weighting function of the system and the weighting of the sensitivity function S, representing the spectral characteristics of the interference and reflecting the shape requirements of the sensitivity function s of the system. In order to effectively suppress the influence of interference, the direct current gain of $W_1(s)$ should be greater than the proportional coefficient of instruction error and the proportional coefficient of interference suppression, so it generally has integral characteristics or high-gain low-pass characteristics. $W_2(s)$ indicates that the norm bound of additive perturbation is determined by the control signal. In order not to increase the order of the controller, it is generally selected as a constant. $W_3(s)$ is a weighted function of the complementary sensitivity function T, representing the norm bound of the multiplicative perturbation, reflecting the

requirement of robust stability. Generally, there should be high-pass filtering characteristics.

According to the transfer function structure diagram. The closed-loop transfer functions from $r(t)$ to $e(t)$, $u(t)$ and $y(t)$ are:

$$\begin{cases} S = (I + GK)^{-1} \\ R = K\,(I + GK)^{-1} \\ T = GK\,(I + GK)^{-1} \end{cases} \tag{10}$$

The standard framework considering the weighted mixed sensitivity problem obtains the input/output relation after introducing the weight function:

$$\begin{bmatrix} W_1 e \\ W_2 u \\ W_3 y \\ e \end{bmatrix} = \begin{bmatrix} W_1 & -W_1 G \\ 0 & W_2 \\ 0 & W_3 G \\ I & -G \end{bmatrix} \begin{bmatrix} r \\ u \end{bmatrix} \tag{11}$$

where, the model expression of generalized controlled object aircraft after weight function is introduced is:

$$P_0 = \begin{bmatrix} W_1 & -W_1 G \\ 0 & W_2 \\ 0 & W_3 G \\ I & -G \end{bmatrix} \tag{12}$$

The closed-loop transfer function matrix of the system from the external input signal (external interference, noise, reference input, etc.) to the output of the controller is:

$$P = \begin{pmatrix} W_1 S \\ W_2 R \\ W_3 T \end{pmatrix} \tag{13}$$

The mixed sensitivity problem is to find a real rational function controller K(s), so that the closed-loop system is stable and satisfies $\|P\|_\infty < 1$.

2) LONGITUDINAL MIXING CONTROLLER DESIGN

In the longitudinal control system of UAVs, robust H_∞ control pitch Angle loop is adopted, that is, the internal and external loop of the longitudinal control system, and the external loop is mainly controlled by the S-plane control method. In the longitudinal control system, the control of the outer loop is mainly to control the height and speed of the UAVs.

Highly loop and speed loop simulation test according to adjust the parameters in the S plane control display curve, parameter setting method here without explanation, which is the parameters k_1 and PD control k_2 works in a similar way, increase the two parameters can accelerate the convergence speed, works in a similar way, the other two parameters are used to reduce the overshoot. After many simulation tests, the final determined control parameters are set as follows: the parameters $k_1 = 0.625$ and $k_2 = 0.6$ controlled by the S-plane of the height control loop are the control parameters that reach the set height most rapidly after parameter setting, and the curve is smooth and there is no overshoot. The parameters $k_1 = 2.775$ and $k_2 = 3.485$ controlled by the S-plane of the speed control loop are the control parameters that reach the optimal control effect of the set speed with smooth curve and no overshoot after parameter setting.

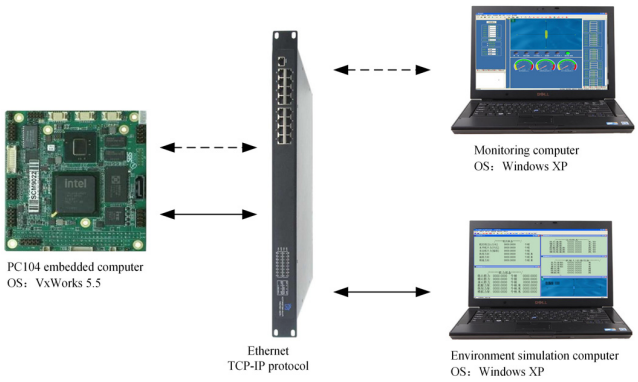

FIGURE 5. Semi-physical simulation system.

MATLAB-based Simulink toolbox, build UAV height control simulation platform. According to the stability of the system and the constraint relationship between the model and the weight function, we designed the test program between the model and the weight function. After running the simulation program and making several adjustments, the three weight functions were finally determined as:

$$W_1(s) = \frac{0.075\,(0.001s + 1)}{s + 0.001}; \quad W_2(s) = 0.1;$$
$$W_3(s) = 0.002\,(s + 0.005)\,.$$

Two Riccati equations were solved with MATLAB robust control toolbox, and the optimal H_∞ controller of the inner loop was obtained as:

$$K_\infty = \frac{81.939(s^2+0.03392s+0.04641)(s^2+4.979s+12.95)}{(s+132.1)(s+0.02984)(s+0.001)(s^2+6.2765s+11.93)}$$

IV. LONGITUDINAL CONTROL OF UAV

The semi-physical simulation system is built as shown in Fig.5. The semi-physical simulation system mainly consists of three parts: PC/104 embedded computer, ground station monitoring computer and environment simulation computer. The environment simulation computer is used to simulate the real environment disturbance, the UAV's motion state and the sensor on board. Both the PC/104 embedded computer and the ground station monitoring computer are the actual equipment used. The only difference between the semi-physical simulation and the real field test is that the external environment interference and sensor measurement data are sent to the PC/104 by the environment simulation computer via Ethernet, and the actuator information is also sent to the environment simulation computer via Ethernet. In order to verify the effectiveness of the controller proposed in this paper, a certain UAV was selected as the research object and compared with H_∞/PD controller and PID controller for comparative simulation test.

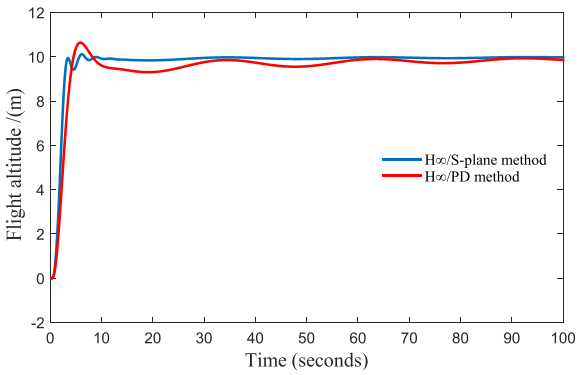

FIGURE 6. Simulation diagram of height without interference.

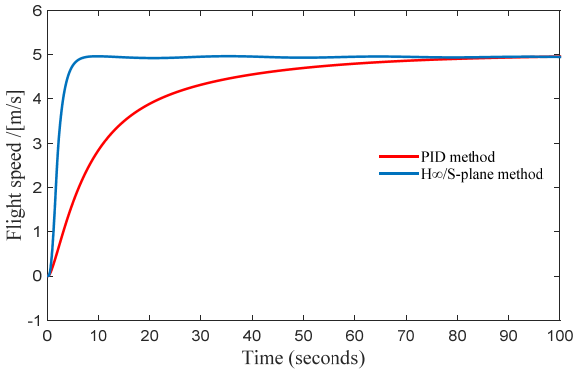

FIGURE 7. Speed simulation diagram without interference.

A. LONGITUDINAL FLIGHT CONTROL WITHOUT EXTERNAL DISTURBANCE

In the simulation experiment, the flight speed of the aircraft is 53.5m/s, and the aircraft model parameters are given in the second part. Given the height signal of the system rising 10m, the curves of the two controllers' changes in height value are obtained by running the simulation model, as shown in Fig.6

As can be seen from the simulation curve, the H_∞/S-plane controller reaches stability around 8s, and the maximum overshot is about 10.2m. The H_∞/PD controller reaches the set height around 10s, and the maximum overshoot is about 10.8m, and there is a certain fluctuation in the whole simulation process.

Because the s plane controller is nonlinear compared to the PD controller, and the output of S-plane controller has higher gain in the initial stage, the S-plane control can reach the set height quickly. In the stability stage, the non-linearity of the S-plane control itself makes its control effect slightly fluctuate. After the introduction of robust H_∞ control, the uncertainty will be judged and corrected, so that the final control effect is relatively stable. After the introduction of H_∞ robust control, the uncertainty of the system will be modified, so that the final control effect will fluctuate. This group of simulation experiments verify that H_∞/S-plane controller has the advantages of fast and high precision in the absence of interference.

The robust H_∞/S-plane controller and PID controller were designed to control the speed control system, and the step signal with the speed increment command of +5m/s was given to the system, and the aircraft speed was increased by 5m/s. The curves of the speed changes of the two control systems were obtained by running the simulation system, as shown in Fig.7.

It can be seen from the simulation curve that the H_∞/S-plane controller reached a stable state at about 10s, and the PID controller reached a stable state at about 80s, which took 8 times longer than that of the H_∞/S-plane controller, fully demonstrating the rapidity of the H_∞/S-plane controller. However, compared with the PID controller, the H_∞/S-plane controller fluctuates a lot in the later stage. This is because the simulation test is carried out under relatively ideal conditions, and there is no simulation of its own error or external environment. As a result, the partial linear and very simple control algorithm of the PID controller has greater advantages after the system is stabilized. In order to enhance the authenticity of the simulation experiment, the influences of interference and parameter perturbation on the control effect are studied in the following simulation experiment.

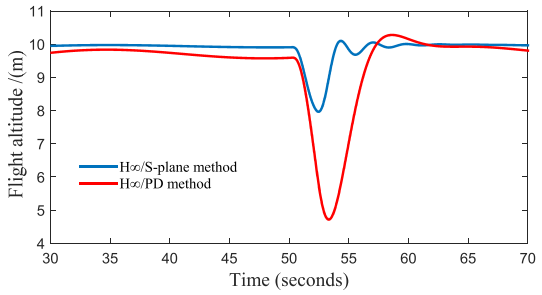

FIGURE 8. Simulation diagram under vertical wind disturbance (Fig.5 30-70S).

B. LONGITUDINAL FLIGHT CONTROL WITH EXTERNAL DISTURBANCE

In the process of flight, the UAV is often affected by the vertical wind, which seriously affects the stability of the UAV. The square wave module in the Simulink toolbox is used to simulate the vertical wind effect in the simulation. In the 50s, add interference, which is a square-wave interference with a cycle of 50s, pulse width of 1 and amplitude of 5. The simulation curves are shown in Fig.8 and Fig.9.

It can be seen from Fig.8 that the disturbance is added after stabilization, and the height change range of H_∞/S-plane controller disturbance is (8.1,10.1) m, and it takes about 8s to reach the original flight control height and maintain the effect of stable flight. When the controller of H_∞/PD was disturbed, the height change range is (5,10.5) m, and it takes about 15s to reach the original flight control height, and there are fluctuations in the subsequent flights. It shows that the fluctuation range controlled by the H_∞/S-plane controller is

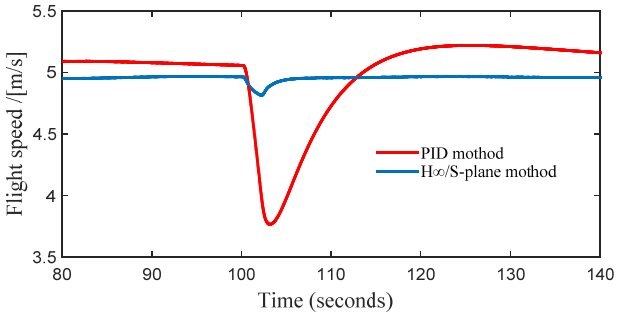

FIGURE 9. Velocity simulation diagram under vertical wind disturbance.

obviously small, and the system quickly achieves stability after the interference disappears through self-adjustment, indicating that it has strong anti-interference ability and fast self-stabilization ability.

Fig.9 shows that the H_∞/S-plane controller controls the speed within the range of (4.8-5.0m/s) with vertical wind disturbance added after stabilization, and the original stable speed is reached after about 5s. The PID controller controls the vertical wind disturbance speed within the range of (3.5-5.1m/s), and it takes about 15s to reach the original stable speed. The results show that the velocity fluctuation of the H_∞/S-plane controller is small and can reach the original stable state quickly, indicating that the control system has strong anti-interference ability and fast self-stabilization ability.

In addition to vertical wind disturbance, the uav may also be disturbed by undirected air flow. Interference can be simulated by the band-limited White Noise module in the Simulink toolbox, which can generate gaussian White Noise with a specified amplitude and can be Limited to a specified time by the timing module. The control results obtained by running the simulation program are shown in Fig. 10 and Fig.11.

Fig.10 shows that the system fluctuation amplitude under the control of the H_∞/S-plane controller in the interference stage is obviously small and the fluctuation is uniform. Although both of them can reach a stable state after the interference disappears, the H_∞/PD controller has a large fluctuation when the system is subject to external interference and its anti-interference ability is poor.

From the local enlarged image of undirected flow disturbance, it can be clearly seen that the H_∞/S-plane controller has a small fluctuation and even change throughout the disturbance time, and the velocity variation range is between 4.96-4.98m/s, that is, the fluctuation range is 0-0.02m/s. However, the PID controller fluctuates greatly and changes unevenly throughout the disturbance time, and the velocity variation range is between 4.95 and 5.10m/s, that is, the fluctuation range is 0-0.15m/s. It can be seen from this that the anti-directional flow disturbance ability of H_∞/S-plane controller is enhanced by 7 times. After the disturbance disappears, the H_∞/S-plane controller will return

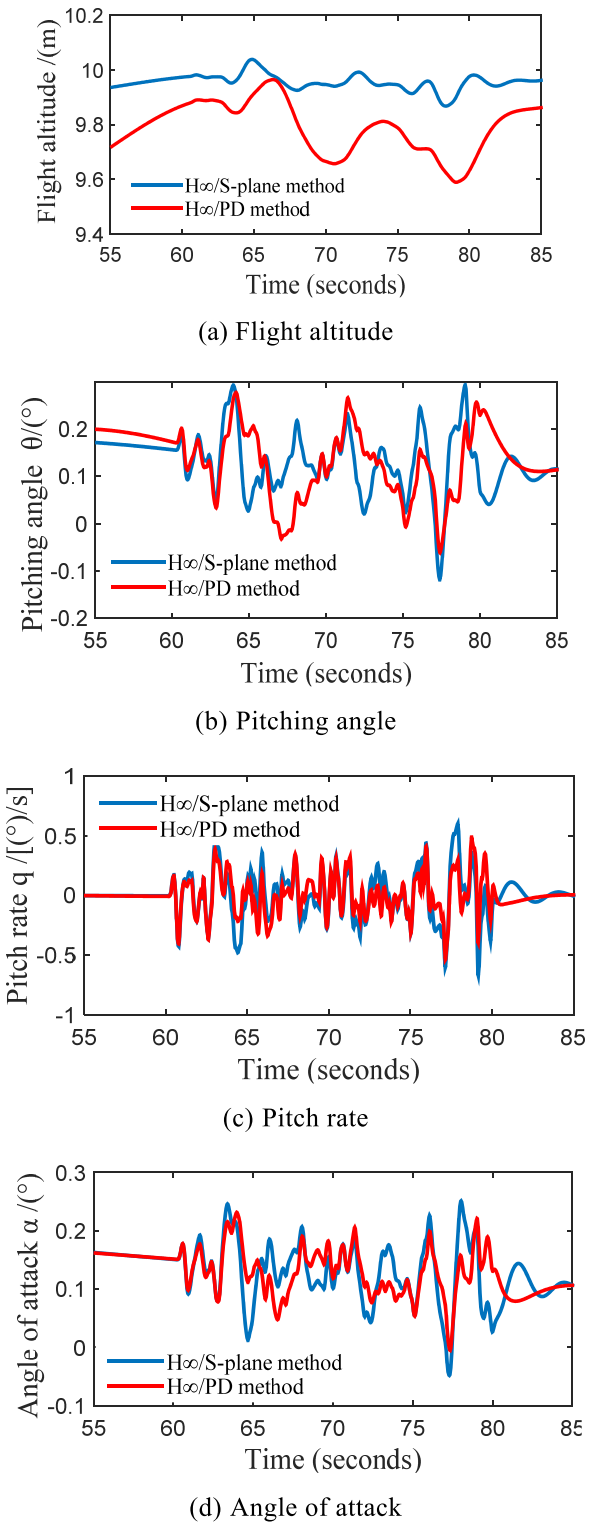

FIGURE 10. Attitude response of aircraft disturbed by undirected airflow in the altitude control system.

to the original stable state after about 3s, while the PID controller will return to the stable state after about 10s after the disturbance disappears. The H_∞/S-plane controller shows its rapidity and strong anti-interference ability.

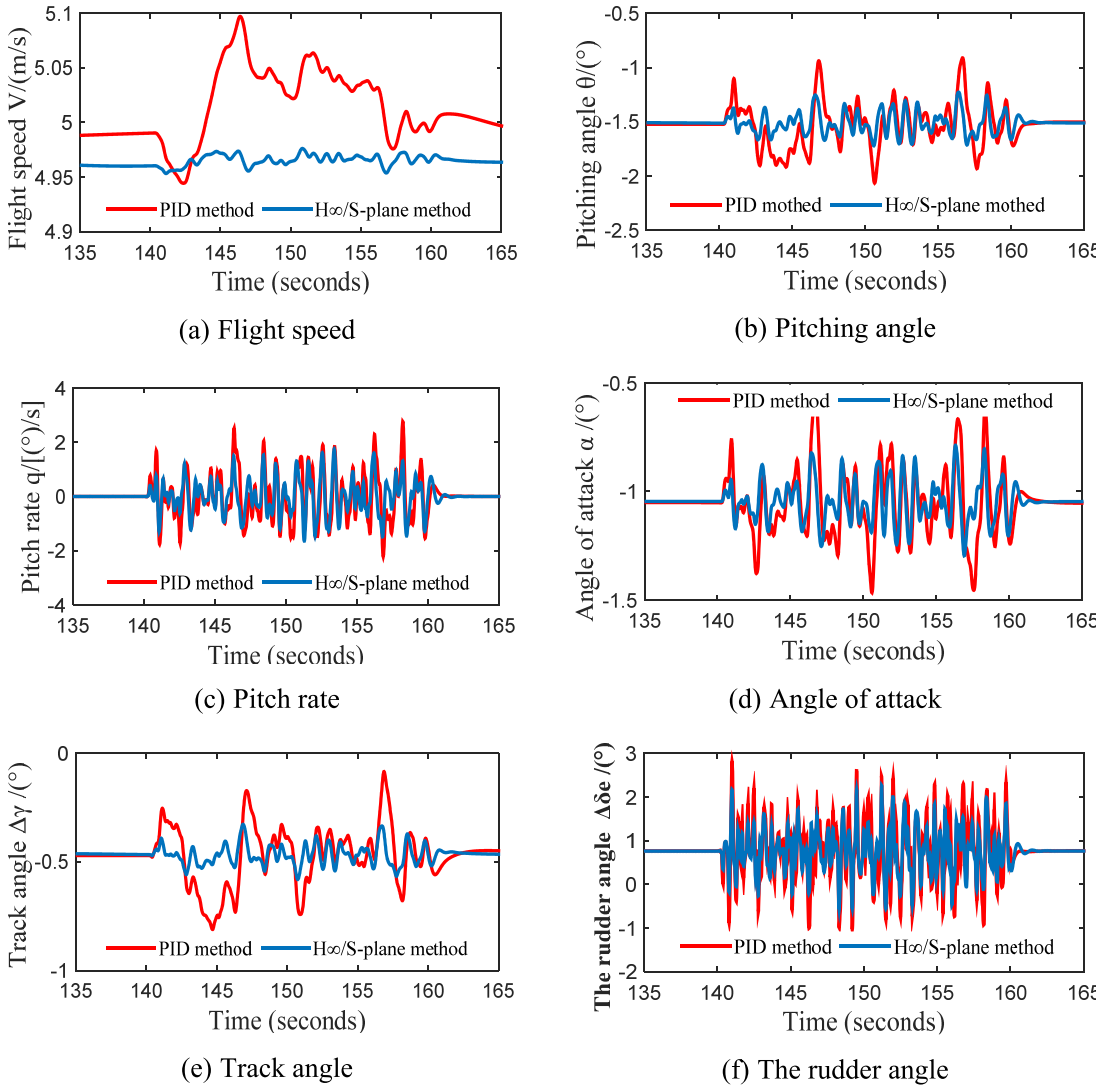

FIGURE 11. Attitude response of an aircraft disturbed by undirected airflow in the speed control system.

V. CONCLUSION

Taking the UAV flight longitudinal control system as the research object, we designed a controller based on H_∞/S-plane controller. The S-plane controller algorithm adopted by the outer loop has a stronger nonlinear control characteristic than PD controller, and the control loop based on the pitch Angle of the inner loop adopted the robust H_∞ controller based on the mixed sensitivity, which improves the system robustness. Simulation experiments were carried out to verify that:

(1) Giving the system instruction, the H_∞/S-plane controller rapidly arrives and remains stable with small overshoot.

(2) Compared with H_∞/PD and PID controllers, the response time of H_∞/S surface model controller decreases by 20% and 87.5% respectively, and the overshoot of flight altitude decreases by 3%. It is shown that H_∞/S planar model controller has better rapidity and stability.

(3) Under external interference, the fluctuation of H_∞/S plane controller is smaller, and the recovery speed of stable state is faster, indicating that H_∞/S-plane controller has strong anti-interference ability and good stability.

REFERENCES

[1] A. Hinas, J. M. Roberts, and F. Gonzalez, "Vision-based target finding and inspection of a ground target using a multirotor UAV system," *Sensors*, vol. 17, no. 12, p. 2929, Dec. 2017.

[2] T. Sankey, J. Donager, J. McVay, and J. B. Sankey, "UAV lidar and hyperspectral fusion for forest monitoring in the southwestern USA," *Remote Sens. Environ.*, vol. 195, pp. 30–34, Jun. 2017.

[3] Q. Gu, D. R. Michanowicz, and C. Jia, "Developing a modular unmanned aerial vehicle (UAV) platform for air pollution profiling," *Sensors*, vol. 18, no. 12, p. 4363, Dec. 2018.

[4] Z. Kunrong, T. He, S. Wu, S. Wang, B. Dai, Q. Yang, and Y. Lei, "Application research of image recognition technology based on CNN in image location of environmental monitoring UAV," *EURASIP J. Image Video Process.*, vol. 2018, p. 150, Dec. 2018.

[5] K. Song, A. Brewer, S. Ahmadian, A. Shankar, C. Detweiler, and A. J. Burgin, "Using unmanned aerial vehicles to sample aquatic ecosystems," *Limnolgy Oceanogr.-Methods*, vol. 15, pp. 1021–1030, Dec. 2017.

[6] J. Sánchez-García, D. G. Reina, and S. L. Toral, "A distributed PSO-based exploration algorithm for a UAV network assisting a disaster scenario," *Future Gener. Comput. Syst.*, vol. 90, pp. 129–148, Jan. 2019.
[7] A. R. Babaei, M. Mortazavi, and M. H. Moradi, "Classical and fuzzy-genetic autopilot design for unmanned aerial vehicles," *Appl. Soft Comput.*, vol. 11, pp. 365–372, Jan. 2011.
[8] A. J. Calise, E. N. Johnson, M. D. Johnson, and J. E. Corban, "Applications of adaptive neural-network control to unmanned aerial vehicles," in *Proc. AIAA/ICAS Int. Air Space Symp. Expo., Next 100 Years*, Dayton, OH, USA, Jul. 2003, pp. 1–10.
[9] S. Sieberling, Q. P. Chu, and J. A. Mulder, "Robust flight control using incremental nonlinear dynamic inversion and angular acceleration prediction," *J. Guid., Control, Dyn.*, vol. 33, pp. 1732–1742, Jun. 2010.
[10] X.-M. Liu and Y.-R. Xu, "S control of automatic underwater vehicles," *Ocean Eng.*, vol. 19, pp. 81–84, Aug. 2001.
[11] L. Zhang, Y.-J. Pang, Y.-M. Su, F.-L. Zhao, and Z.-B. Qin, "Expert S-surface control for autonomous underwater vehicles," *J. Mar. Sci. Appl.*, vol. 7, no. 4, pp. 236–242, 2008.
[12] R. Wang, Z. Zhou, and Y. H. F. Shen, "Flying-wing UAV landing control and simulation based on mixed H_2/H_∞," in *Proc. Int. Conf. Mechatronics Automat.*, Aug. 2007, pp. 1523–1528.
[13] D. Gadewadikar, J. Lewis, K. Subbara, and B. M. Chen, "Attitude control system design for unmanned aerial vehicles using H-infinity and loop-shaping methods," in *Proc. IEEE Int. Conf. Control Automat.*, May/Jun. 2007, pp. 1174–1179.
[14] S. Yushan, W. Lei, L. Yueming, L. Liwei, and Z. Guocheng, "S plane control based on parameters optimization with simulated annealing for underwater vehicle," in *Proc. Int. Conf. Electron. Mech. Eng. Inf. Technol. (EMEIT)*, Aug. 2011, pp. 552–556.
[15] Y.-M. Li, Y.-J. Pang, and L. Wan, "Adaptive S plane control for autonomous underwater vehicle," *J. Shanghai Jiaotong Univ.*, vol. 46, no. 2, pp. 195–200, Feb. 2012.
[16] A. Mahmood, Y. Kim, and J. Park, "Robust H_∞ autopilot design for agile missile with time-varying parameters," *IEEE Trans. Aerosp. Electron. Syst.*, vol. 50, no. 4, pp. 3082-3089, Oct. 2014.
[17] R. Wang, Z. Zhou, and Y. H. Shen, "Flying-wing UAV landing control and simulation based on mixed H_2/H_∞," in *Proc. Int. Conf. Mechatronics Automat.*, Aug. 2007, pp. 1523–1528.
[18] T. Lee, M. Leok, and N. H. McClamroch, "Nonlinear robust tracking control of a quadrotor UAV on SE(3)," in *Proc. Amer. Control Conf. (ACC)*, 2012, pp. 4649–4654.
[19] D. J. Walker, B. J. Manimala, M. Voskuijl, and A. W. Gubbels, "Multivariable control of the bell 412 helicopter," in *Proc. 45th IEEE Conf. Decis. Control*, San Diego, CA, USA, Dec. 2006, pp. 1527–1532.
[20] F. Santoso, M. Liu, and G. Egan, "H_2 and H_∞ robust autopilot synthesis for longitudinal flight of a special unmanned aerial vehicle: A comparative study," *IET Control Theory Appl.*, vol. 2, no. 7, pp. 583–594, Jul. 2008.

XINGCHENG ZHAO received the B.S. degree in aircraft design and engineering from the College of Mechatronic Engineering, North University of China, in 2016, where he has been a Postgraduate Student of UAV (Unmanned Aerial Vehicle) flight control, since 2016. The flight control research work is carried out in the UAV Innovation Laboratory, North University of China. He has published four academic papers. His research interests include UAV, control systems, and navigation systems. He received the Excellent Paper Award.

MEINI YUAN received the Ph.D. degree from Northwestern Polytechnical University, in 2009. She is currently a Professor and a Doctoral Supervisor with the College of Mechatronic Engineering, North University of China. She is in charge of the Doctoral Programs Fund of the Ministry of Education (20101420120006), Shanxi Natural Resources Fund (2012011019-1), National Natural Science Foundation of China (51201155), National Solidification Key Laboratory Innovation Fund (521030102-0400-w016133), and Postdoctoral Fund (BP201004). She has participated in the completion of Aviation Fund (04G53044), "Eleventh Five-Year" pre-research and the National Natural Science Foundation of China (50871086), and a number of projects. She edited one textbook and one monograph of the 12th Five-Year Plan at the provincial and ministerial level. She had an application for a utility model patent. She has published more than 30 papers in domestic and foreign journals, and more than 20 papers have been included in SCI and EI. In recent years, She has been involved in the teaching and research of integrated design of aviation structure, dynamics and control of aircraft structure, and mechanics mechanism of fracture and damage.

PENGYUN CHENG received the B.S. and Ph.D. degrees in design and construction of naval architecture and ocean structure from Harbin Engineering University, Harbin, China, in 2010 and 2016, respectively. Since 2016, he has been a Lecturer with the College of Mechatronic Engineering, North University of China. His research interests include the autonomous control and navigation technology of unmanned vehicle, optical target recognition, and tracking.

LE XIN received the B.S. degree in aircraft manufacturing engineering from the College of Mechatronic Engineering, North University of China, in 2017, where he has been a Graduate Student majoring in aerospace manufacturing engineering, since 2017. During this period, he participated in the design and manufacture of UAV in the UAV Innovation Laboratory, North University of China. He published two academic papers and holds three patents.

LEIBIN YAO received the B.S. degree in detection, guidance and control technology from the College of Mechatronic Engineering, North University of China, in 2016, where he has been a Graduate Student of mechanical engineering, since 2017.